

Development of an Intelligent System for Cooling Rate and Fill Control in GMAW

Carolyn J. Einerson, Herschel B. Smartt, John A. Johnson, Paul J. Taylor

Idaho National Engineering Laboratory
Idaho Falls, Idaho

Kevin L. Moore

*Idaho State University
Pocatello, Idaho

J EGG-M--92381

DE92 017849

Abstract

A control strategy for gas metal arc welding (GMAW) is developed in which the welding system detects certain existing conditions and adjusts the process in accordance to pre-specified rules. This strategy is used to control the reinforcement and weld bead centerline cooling rate during welding. Relationships between heat and mass transfer rates to the base metal and the required electrode speed and welding speed for specific open circuit voltages are taught to a artificial neural network. Control rules are programmed into a fuzzy logic system.

TRADITIONAL CONTROL OF THE GMAW PROCESS is based on the use of explicit welding procedures detailing allowable parameter ranges on a pass by pass basis for a given weld. The present work is an exploration of a completely different approach to welding control.

In previous work (1) an approach was developed to control the GMAW process based on the recognition that the process is a source of heat and mass transferred to the base metal; melting of the base metal, dilution of the filler metal, solidification of the weld bead, microstructural development in the weld bead and heat affected zone, physical properties development, and thermomechanical distortion and residual stresses in the weldment all follow from the heat and mass transferred by the process to the weld. Control of the process should then involve sensing of desired weld characteristics, determination of required heat and mass transfer rates, and control of heat and mass transfer rates.

In this work the objectives are to produce welds having desired weld bead reinforcements while maintaining the weld bead centerline cooling rate at preselected values. The need for this specific control is related to fabrication requirements for specific types of pressure vessels.

The control strategy involves measuring weld joint transverse cross-sectional area ahead of the welding torch and the weld bead centerline cooling rate behind the weld pool, both by means of video (2), calculating the required process parameters necessary to obtain the needed heat and mass transfer rates (in appropriate dimensions) by means of an artificial neural network, and controlling the heat transfer rate by means of a fuzzy logic controller (3).

The result is a welding machine that senses the welding conditions and responds to those conditions on the basis of logical rules, as opposed to producing a weld based on a specific procedure.

Welding System

The welding hardware is shown in block diagram in Figure 1. The welding power supply is a Philips 450 A PZ 2351/60. The welding head is run by a Hewlett-Packard series 9000, model 236 computer and associated hardware. The weld joint transverse cross-sectional area is imaged by a Pulnix TM-540 ccd-camera. A Melles Griot HeNe laser is used to generate a light stripe across the weld joint. The weld bead is imaged by a Pulnix TM-80 ccd-camera. Video images are digitized by a Data Translation QuickCapture frame grabber board, installed in a Macintosh IIfx computer. Analog output signals are sent from the Macintosh computer to the welding machine by a National Instruments NB-MIO-16X multifunction board or a NB-AO-6 analog output board.

Software

The system software integrates the incoming data from the sensors with an intelligent control scheme to make decisions about changes in the process. The system consists of a Macintosh IIfx computer with a data acquisition board

MASTER

DISTRIBUTION OF THIS DOCUMENT IS UNLIMITED

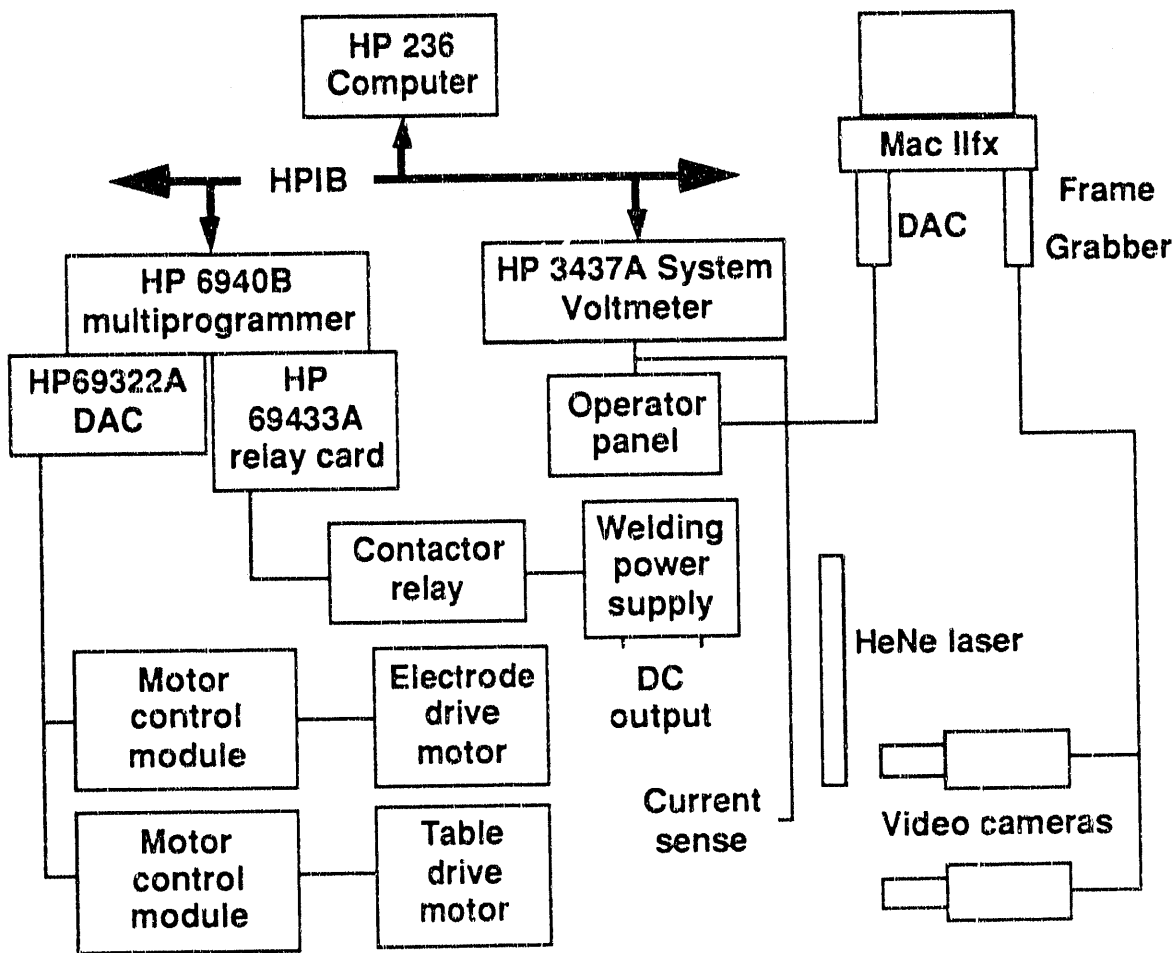


Figure 1. Diagram of welding system components.

to acquire images from the cameras and send analog output to the motor boards. The block diagram shown in Figure 2 illustrates the process. Images from the frame grabber are processed by the computer to calculate the area of the joint being welded, Figure 3, and the cooling rate of the weldment directly behind the torch, Figure 4. The measured cooling rate is compared to the cooling rate setpoint, and this error, along with the measured joint geometry, is processed by the fuzzy logic controller to make decisions regarding changes in heat input and reinforcement. Although information regarding the joint geometry is being processed, the software is presently configured to make control decisions based only on the cooling rate error. An updated desired heat input and reinforcement are used as input to a neural network to calculate the required wire feed speed and weld speed. The neural network was previously trained over a set of experimental data to provide the functional relationship between the desired heat input and reinforcement and the required wire feed speed and weld speed. These are sent to the output board and converted to voltages for the motor control boards. Images acquired during the process may be displayed on the monitor at any time to check camera position.

Experimental Procedure

Welds were made on type A-36 steel plate in both bead on plate and bead in groove configurations. Nominal parameters are given in Table 1.

Table I. Welding Parameters.	
Open-Circuit Voltage	29.0 V
Electrode Speed	150- 220 mm/s
Contact-Tip-to-Workpiece	15.9 mm
Travel Speed	1.0 - 4.0 mm/s
Shielding Gas	Ar - 2% O
Electrode Composition	AWS A5.18, ER70S-3
Electrode Diameter	0.889 mm
Power-Supply Slope	0.004 V/A
Shield-gas Flow	14.2 L/min

Calibration

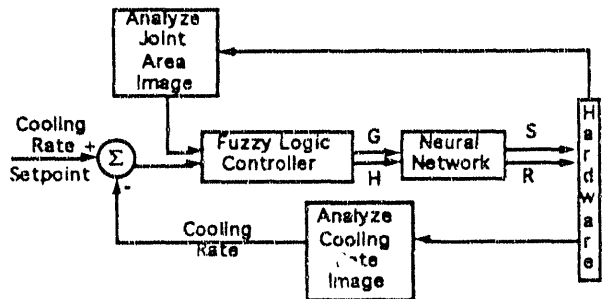


Figure 2. Process control scheme block diagram, where G is the reinforcement, H is heat input, S is electrode speed, and R is travel speed.

Heat transfer efficiency from the GMAW process to the base metal has been determined in prior work to be nominally 85% (4). Calibration of weld joint transverse cross-sectional area measurements involved a combination of imaging of a steel machinists rule on the base metal surface for calibration of linear measurements and measurement of machined weld joint models for which the transverse cross-sectional area was measured by digital calipers.

Weld bead cooling rate measurements were calibrated by means of a black body source. The lowest temperature measurable by the CCD camera at 638 nm wavelength is nominally 1000 °C. An upper temperature was estimated by noting that the weld pool liquid-solid interface, visible in the images, was at a temperature of approximately 1425 °C. This corresponded to a pixel intensity of about 220 (in a 0-256 range) for a camera lens aperture of f/4.0.

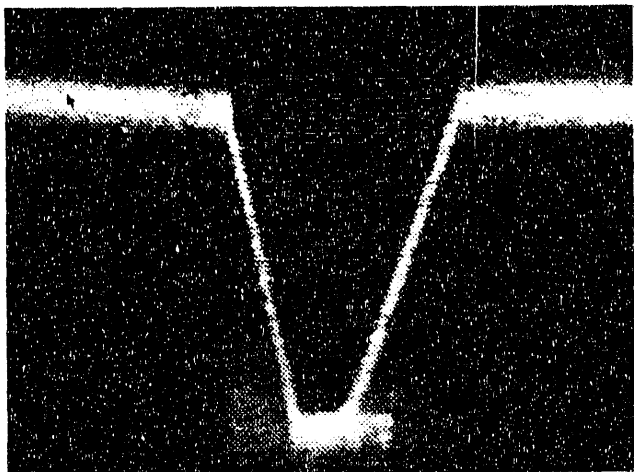


Figure 3. Video image of weld joint showing measurement scans of laser line.

Discussion

The weld joint transverse cross-sectional area measurements are made from images of the weld joint with a laser stripe passing through the field of view. Because the laser stripe is at approximately a 45° angle to the base metal top surface, the intersection of the laser stripe with the base metal surface is a measure of the vertical height of the weld joint. The image analysis algorithm first locates the top surface of the base metal to the left and right of the joint. This is done by taking vertical scans from the top of the image down until the increased intensity of the laser stripe is detected; these two scans are shown in Figure 3. A similar scan, not shown, is made in the center of the image to find the bottom of the weld joint. Then, starting from the center of the image at a location three image scan lines below the top of the base metal, horizontal searches are made to the left and the right to locate the walls of the weld joint. Consecutive searches are made at intervals of five image scan lines until the bottom of the weld joint is reached. The resulting scans are shown in Figure 3. Knowing the horizontal lengths of these scan distances and the vertical height between them, the weld joint transverse cross-sectional area is estimated by means of Simpson's integration rule.

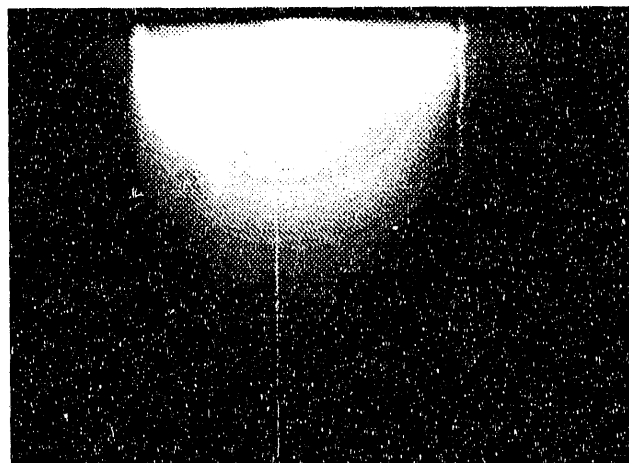


Figure 4. Video image of weld bead behind pool, showing scan location for cooling rate measurement.

Measurement of the weld bead centerline cooling rate involves acquiring pixel intensity data from a vertical scan line from the image approximately centered on the weld bead, Figure 4. The intensity data is sent to a procedure that extracts intensities between pixel gray levels of 150 to 100. These values are then sent to a procedure that obtains a best-fit, straight-line approximation of the data, from which a value for the derivative of pixel intensity with respect to distance along the weld bead is calculated. This value is then converted to the derivative of temperature with respect to time by means of multiplying by the derivative of pixel intensity with respect to temperature and dividing by the present value for welding speed.

The values for required reinforcement and weld bead cooling rate, are then sent via a fuzzy logic controller to an artificial neural network that maps the electrode speed and welding speed for a given power supply open circuit voltage as a function of reinforcement and heat input per unit length. The fuzzy logic controller adjusts the heat input per unit length as required to obtain the desired weld bead cooling rate.

The heat input to the neural network was calculated using a two-rule, fuzzy-logic system (5) that simulated a proportional controller (3). The rules are:

If the COOLING RATE is LOW, then the CHANGE in HEAT INPUT is NEGATIVE.

If the COOLING RATE is HIGH, then the CHANGE in HEAT INPUT is POSITIVE.

We use a nonstandard fuzzy-logic system to implement these rules (5). For this simple case with no ANDs or ORs, the calculation reduces to multiplying the value of the membership functions for the cooling rate, LOW and HIGH, by an output action to obtain the change in the heat input, NEGATIVE and POSITIVE, for each rule and then adding the result to obtain the total change in heat input. No complicated defuzzification is required since the output membership functions are crisp. Therefore, membership functions are required only for the antecedent, the cooling rate HIGH and LOW. These are taken to be linear functions

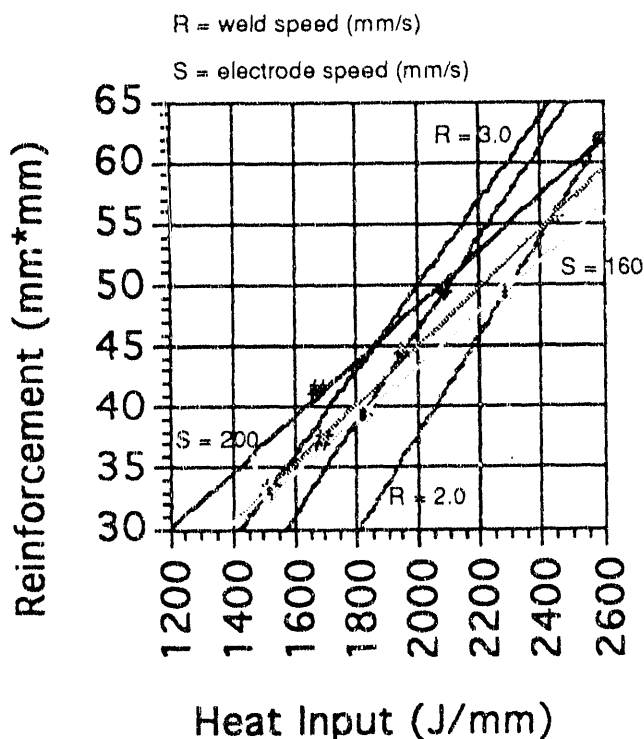


Figure 5 Experimental data set used to train artificial neural network.

with HIGH increasing from zero at $-50\text{ }^{\circ}\text{C/s}$ (below the set point) to one at $+50\text{ }^{\circ}\text{C/s}$ (above the set point). The membership function for LOW is just the reverse, decreasing from one to zero over the same range. The crisp values of the change in heat input corresponding to NEGATIVE and POSITIVE are $\pm 3\text{ J/mm}$. For example, consider the case where the cooling rate is $25\text{ }^{\circ}\text{C/s}$ below the set point. Then the value of the membership function LOW is 0.75 and High is 0.25. Multiplying by the respective output actions for each rule gives -2.25 J/mm and $+0.75\text{ J/mm}$ for a total of -1.50 J/mm .

The calculations are done in a normalized space where the range of all the membership functions are from zero to one. This makes changing the range membership functions easy since only the normalization needs to be changed and the logic remains the same.

An artificial neural network was trained using the backpropagation method (6) to learn the functional relationship between the heat input and reinforcement and the wire and welding speeds. A set of experimental data, Figure 5, was obtained by setting the wire and welding speeds prior to welding, measuring the current during welding, and subsequently calculating the reinforcement and heat input. The arc efficiency used in the heat input calculation was measured in prior work (4). The network is taught the inverse of the measured relationship by using the heat input and reinforcement as inputs to the network and the weld and electrode speeds as outputs. The hidden layer consists of 20 hidden nodes with biases and a sigmoidal activation function is used in the hidden layer only. The trained network is implemented in the overall control scheme to give the wire and welding speeds for the process.

A result of a controlled welding run where the reinforcement setpoint is 42 mm^2 and the cooling rate setpoint was $150\text{ }^{\circ}\text{C/s}$ is shown in Figure 6. The heat input per unit length to the weldment is shown in Figure 7, calculated from process parameters assuming an average 85% heat transfer efficiency.

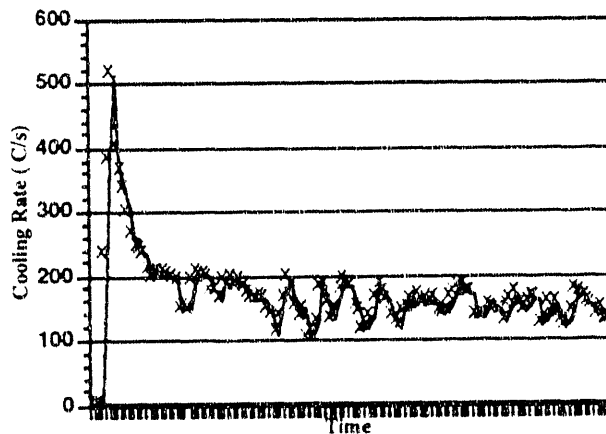


Figure 6. Weld bead centerline cooling rate.

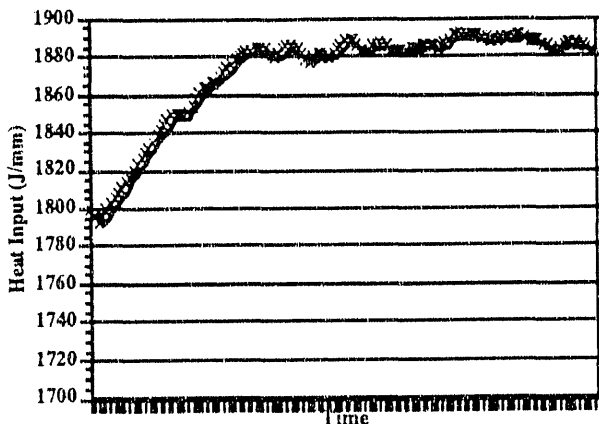


Figure 7. Weldment heat input as a function of time, for the weld shown in Figure 6.

Conclusions

An intelligent control scheme has been developed that produces welds having desired weld bead reinforcements while maintaining preselected weld bead centerline cooling rates. On-line processed video images provide weld joint area and bead centerline cooling rates. This information is utilized by a fuzzy logic controller and an artificial neural network to appropriately modify process parameters.

Results indicate that the control strategy used in this work, based on feedback control of cooling rate in combination with feed forward control of reinforcement has potential for application to welding fabrication.

Acknowledgments

Appreciation is expressed to U.S. Wallace and Nancy Carlson for their support. This work was supported by the U.S. Department of Energy, Office of Energy Research, Office of Basic Energy Sciences Under DOE Contract No. DE-AC07-76ID01570.

References

1. H. B. Smartt, C. J. Einerson, A. D. Watkins, R. A. Morris, in Advances in Welding Science and Technology, ASM, 461-465. (1986)
2. P. L. Taylor, A. D. Watkins, E. D. Larsen, H. B. Smartt, in Proceedings 3rd Int. Conf. on Trends in Welding Research, Gatlinburg, TN, June, 1992.
3. H. B. Smartt, J. A. Johnson, C. J. Einerson, and G. A. Cordes, in Intelligent Engin. Systems Through Artificial Neural Networks, ASME (1991)
4. A. D. Watkins, MS Thesis, Univ. of Idaho, 1989.
5. T. Takagi and M. Sugeno, IEEE Trans. Systems, Man, and Cybernetics SMMC 15, 116-132 (1985)
6. D. E. Rumelhart, G. E. Hinton, and R. J. Williams, "Learning Internal Representations by Error Propagation," Parallel Distributed Processing: Explorations in the Microstructures of Cognition, Vol. 1, ed. D. E. Rumelhart and J. L. McClelland, MIT Press, Cambridge, MA, pp. 318-362.

DISCLAIMER

This report was prepared as an account of work sponsored by an agency of the United States Government. Neither the United States Government nor any agency thereof, nor any of their employees, makes any warranty, express or implied, or assumes any legal liability or responsibility for the accuracy, completeness, or usefulness of any information, apparatus, product, or process disclosed, or represents that its use would not infringe privately owned rights. Reference herein to any specific commercial product, process, or service by trade name, trademark, manufacturer, or otherwise does not necessarily constitute or imply its endorsement, recommendation, or favoring by the United States Government or any agency thereof. The views and opinions of authors expressed herein do not necessarily state or reflect those of the United States Government or any agency thereof.

END

DATE
FILMED
9/17/1922

